Ryanodine receptor type 2 deficiency changes excitation–contraction coupling and membrane potential in urinary bladder smooth muscle

Shingo Hotta[1], Kozo Morimura[1], Susumu Ohya[1], Katsuhiko Muraki[1,2], Hiroshi Takeshima[3] and Yuji Imaizumi[1]

[1]*Department of Molecular and Cellular Pharmacology Graduate School of Pharmaceutical Science, Nagoya City University, Nagoya, Japan*
[2]*Cell Signalling & Ion Channel Research Group, Cellular Pharmacology, School of Pharmacy, Aichigakuin University, Nagoya, Japan*
[3]*Department of Biological Chemistry, Kyoto University Graduate School of Pharmaceutical Sciences, Kyoto, Japan*

The possibility that the ryanodine receptor type 2 (RyR2) can function as the major Ca^{2+}-induced Ca^{2+} release (CICR) channel in excitation–contraction (E-C) coupling was examined in smooth muscle cells (SMCs) isolated from urinary bladder (UB) of RyR2 heterozygous KO mice ($RyR2^{+/-}$). RyR2 mRNA expression in UB from $RyR2^{+/-}$ was much lower than that in wild-type ($RyR2^{+/+}$). In single UBSMCs from $RyR2^{+/+}$, membrane depolarization under voltage clamp initially induced several local Ca^{2+} transients (hot spots) in peripheral areas of the cell. Then, Ca^{2+} waves spread from Ca^{2+} hot spots to other areas of the myocyte. The number of Ca^{2+} hot spots elicited by a short depolarization (< 20 ms) in UBSMCs of $RyR2^{+/-}$ was significantly smaller than in those of $RyR2^{+/+}$. The force development induced either by direct electrical stimulation or by 10 μM acetylcholine in tissue segments of $RyR2^{+/-}$ was smaller than and comparable to those in $RyR2^{+/+}$, respectively. The frequency of spontaneous transient outward currents in single myocytes and the membrane depolarization by 1 μM paxilline in tissue segments from $RyR2^{+/-}$ were significantly lower and smaller than those in $RyR2^{+/+}$, respectively. The urination frequency and volume per voiding in $RyR2^{+/-}$ were significantly increased and reduced, respectively, compared with $RyR2^{+/+}$. In conclusion, RyR2 plays a crucial role in the regulation of CICR during E-C coupling and also in the regulation of resting membrane potential, presumably via the modulation of Ca^{2+}-dependent K^+ channel activity in UBSMCs and, thereby, has a pivotal role in the control of bladder activity.

(Resubmitted 11 February 2007; accepted after revision 8 March 2007; first published online 15 March 2007)
Corresponding author Y. Imaizumi: Department of Molecular and Cellular Pharmacology, Graduate School of Pharmaceutical Science, Nagoya City University, 3-1 Tanabedori, Mizuhoku, Nagoya 467-8603, Japan.
Email: yimaizum@phar.nagoya-cu.ac.jp

The ryanodine receptor (RyR) is one of the major Ca^{2+} release channels in endo- and sarcoplasmic reticulum (ER and SR). Previous cDNA cloning studies have defined three subtypes of RyR (RyR1, RyR2 and RyR3) that are encoded by distinct genes in vertebrates (Meissner, 1994; Laporte *et al.* 2004). RyR1 is expressed abundantly in skeletal muscle cells (Takeshima *et al.* 1989). RyR2 is found predominantly in cardiac muscle cells, although it is expressed at moderate levels in most excitable cells (Nakai *et al.* 1990; Otsu *et al.* 1990). RyR3 is expressed at low levels in a wide variety of cell types including most excitable cells and certain non-excitable cells (Giannini *et al.* 1992; Hakamata *et al.* 1992). Among these three types of RyRs, RyR2 is expressed in cardiac muscle, smooth muscle and brain, and is considered to be the channel mainly responsible for the Ca^{2+}-induced Ca^{2+} release (CICR) mechanism (Fabiato, 1985; Iino, 1989). In cardiac ventricular myocytes, an action potential evokes opening of voltage-dependent Ca^{2+} channels (VDCCs) and Ca^{2+} influx into myoplasm, which activates RyR2 in junctional SR to release Ca^{2+} (Fabiato, 1983). RyR2 is considered to be an essential molecule for CICR in the excitation–contraction coupling in cardiac ventricular myocytes. RyR2 gene deletion in mice ($RyR2^{-/-}$) results in embryonic lethality in homozygotes. Specifically, the progeny die at approximately embryonic day 10 as a result of cardiac arrest, which is presumably due to SR Ca^{2+} overloading and resulting dysfunction of intracellular organelle in cardiac myocytes (Takeshima *et al.* 1998).

This paper has online supplemental material.

DOI: 10.1113/jphysiol.2007.130302

In contrast to cardiac myocytes, in many types of smooth muscles (SMs), inositol 1,4,5-trisphosphate (IP_3)-induced Ca^{2+} release (IICR) by formation of IP_3 via GTP binding protein coupled receptor stimulation and the subsequent activation of phospholipase C is more common than CICR. The contribution of CICR to E-C coupling widely varies between SM types. CICR making a substantial contribution has been reported only in highly excitable SMs such as urinary bladder (UB) (Ganitkevich & Isenberg, 1992; Imaizumi *et al.* 1998; Hashitani *et al.* 2000) and vas deferens (Imaizumi *et al.* 1998), but not portal vein (Kamishima & McCarron, 1996). It has been suggested, however, that the coupling between VDCC and RyR is relatively weak even in UBSM cells (UBSMCs) of the rabbit (Collier *et al.* 2000). There are also reports suggesting that CICR may not be involved effectively in E-C coupling in guinea-pig UB (Herrera *et al.* 2000; Hashitani & Brading, 2003) and rat and human uterus (Taggart & Wray, 1998; Kupittayanant *et al.* 2002). In a previous study, we have demonstrated that CICR through RyR is essential for E-C coupling triggered by an evoked action potential in mouse UBSMCs. We also showed that the cross talk of CICR with IICR by IP_3 formation may not be involved in the E-C coupling under these conditions (Morimura *et al.* 2006).

In many types of SMs, the expression levels of RyR2 are much lower than that in cardiac myocytes (Nakai *et al.* 1990) and the expression of RyR3 has been suggested to be lower than but occasionally comparable to that of RyR2 (Chamber *et al.* 1999; Sanders, 2001). Subtype-specific contributions of RyR2 and/or RyR3 to CICR during E-C coupling in SMs are, however, not well characterized. The substantial contribution of RyR2 to Ca^{2+} spark generation has been suggested only by the indirect evidence that Ca^{2+} sparks were altered in SM myocytes from FKBP12.6 deficient mice (Wang *et al.* 2004). In addition, it has been reported that the Ca^{2+} mobilization in UBSM myocytes from RyR3 homozygous KO mice is not significantly different from that in wild-type mice (Ji *et al.* 2004). In contrast, Ca^{2+} spark/spontaneous transient outward current (STOC) frequency was significantly increased in cerebral artery SMCs of RyR3 KO mice (Löhn *et al.* 2001). Consistent with the latter finding in $RyR3^{-/-}$, it has been suggested recently that an alternative splice variant of RyR3, which works as a dominant negative construct, is predominantly expressed in SM tissues, including mouse UB (Dabertrand *et al.* 2006).

The present study was undertaken to elucidate the functional significance of RyR2 in E-C coupling in UBSM using RyR2 heterozygous KO mice ($RyR2^{+/-}$), in which the functional expression of RyR2 may be substantially reduced. The present results provide direct evidence for an obligatory role of RyR2 in E-C coupling, and also strongly suggest that RyR2 activity can regulate resting membrane potential in UBSM through modulation of Ca^{2+} activated K^+ channel activity.

Methods

PCR Genotyping of $RyR2^{+/-}$ mice

Generation of the RyR2 knockout mice has been reported previously (Takeshima *et al.* 1998). To determine the genotypes of the mutant mice, the polymerase chain reaction (PCR) was carried out using primers from the genomic sequence: forward primer (Ex1-P6D, 25 mer: GAGCCCCTAGAACATCCTGGTTAGC) and reverse primer (AInt-668, 25 mer: GCACCCTGG-GGGCAGCCTTCTCAGC) (Takeshima *et al.* 1998). Amplified DNAs were analysed on 1.5% agarose gels.

RNA extraction and RT-PCR

Eight- to ten-week-old male and female mice were anaesthetized with ether and killed by decapitation. All experiments were carried out in accordance with the guiding principles for the care and use of laboratory animals of The Science and International Affairs Bureau of the Japanese Ministry of Education, Culture, Sports, Science and Technology, and also with the approval of the ethics committee at Nagoya City University. Total RNAs were extracted from homogenates of aorta, brain, colon, diaphragm, heart, ileum, stomach, urinary bladder, uterus or vas deferens by the acid guanidium thiocyanate–phenol method following digestion with RNase-free DNase, and RT was performed with a Gibco BRL protocol as previously reported (Ohya *et al.* 1997). The designed primers are shown in Table 1. The amplification profiles for these primer pairs were as follow: 95°C for 10 min to activate the AmpliTaq polymerase, then 32 cycles of 9°C for 15 s and 60°C for 1 min, performed in a GeneAmp 2400 thermal cycler (PE Applied Biosystems, USA).

Quantitative PCR

Real-time quantitative PCR was performed with the use of SYBR Green Chemistry on an ABI 7000 sequence detector (Applied Biosystems, Foster City, CA, USA). Standard curves were generated for the constitutively expressed glyceraldehyde-3-phosphate dehydrogenase (GAPDH) from regression analysis of the mean values of RT-PCRs for the $\log_{10}$ diluted cDNA. Unknown quantities relative to the standard curve for a particular set of primers were calculated, yielding transcriptional quantification of gene products relative to the endogenous standard (GAPDH). Each cDNA sample was tested in triplicate. The specific primers used in this series of experiments are listed in Table 1.

Cell isolation

Male mice between 8 and 10 weeks old were used in these experiments. Single smooth muscle cells (SMCs) were enzymatically isolated from the urinary bladder

Table 1. Oligonucleotide sequence of primers used for quantitative PCR

	Primer sequence	Primer site	Product length (bp)	GenBank accession no.
RyR1	(+): 5′-ATTACAGAGCAGCCCGAGGAT-3′ (−): 5′-AGAACCTTCCGCTTGACAAACT-3′	450–470 562–541	113	X83932
RyR2	(+): 5′-CTTCGATGTTGGCCTTCAAGAG-3′ (−): 5′-AGAACCTTCCGCTTGACAAACT-3′	432–453 533–512	102	NM_023868
RyR3	(+): 5′-GGCCAAGAACATCAGAGTGACTAA-3′ (−): 5′-TCACTTCTGCCCTGTCAGTTTC-3′	385–408 485–464	101	AF111166
VDCCα1c	(+): 5′-ACCTGGAACGAGTGGAGTATCTCTT-3′ (−): 5′-TCCAACCATTGCGGAGGTAA-3′	473–497 586–567	114	NM_009781
VDCCβ2	(+): 5′-CAGGGTTCTCAAGGTGATCAAAG-3′ (−): 5′-GAGGAACGGTGTTGGGATTTT-3′	1477–1499 1586–1566	110	NM_023116
VDCCβ3	(+): 5′-CTCCCATCATCGTCTTTGTCAA-3′ (−): 5′-GCTTATCGTACGCCATCATCTG-3′	913–934 1029–1008	117	NM_007581
BKα	(+): 5′-GCATTGGTGCCCTCGTAATATAC-3′ (−): 5′-CGTTGAAAGCCATGTCGATCT-3′	1308–1330 1412–1392	105	NM_010610
SK2	(+): 5′-AACCACCGCAGATGTGGATATT-3′ (−): 5′-GGCATCGGTGAAAAGTTTGC-3′	732–753 834–815	103	AA692872
SK4/IK	(+): 5′-CGTGCACAACTTCATGATGGA-3′ (−): 5′-TTCCTTCGAGTGTGCTTGTAGTACA-3′	885–905 990–966	106	AF072884
JP2	(+): 5′-AAGAAGGGCCGTAAGGAAGT-3′ (−): 5′-GGCCGATGTTCAGCAAGATC-3′	2378–2397 2483–2464	106	AB024447
SERCA2	(+): 5′-AGTTCATCCGCTACCTCATCTCA-3′ (−): 5′-CACCAGATTGACCCAGAGTAACTG-3′	2483–2505 2601–2578	119	AJ223584
FKBP1a	(+): 5′-ACTAGGCAAGCAGGAGGTGA-3′ (−): 5′-CTCCATAGGCATAGTCTGAGGAGAT-3′	247–266 350–326	104	NM_008019
FKBP1b	(+): 5′-GAGACGGAAGGACATTCCCTAAG-3′ (−): 5′-CCCTTTTGAAGCATTCCTGTGT-3′	32–54 101–80	70	NM_016863
InsP_3R1	(+) 5′-GGACCGGACAATGGAACAGAT-3′ (−) 5′-CATCCCGCTCTGTGGTGTAAT-3′	6928–6948 7008–7028	101	NM_010585
Sorcin	(+) 5′-TGGACAGGACGGACAAATTGA-3′ (−) 5′-GGCGACAAGTCTCCAGGTTAAA-3′	84–104 184–163	101	NM_025618
GAPDH	(+): 5′-CATGGCCTTCCGTGTTCCT-3′ (−): 5′-CCTGCTTCACCACCTTCTTGA-3′	730–748 833–813	104	M32599

+, sense; –, antisense.

(UB) using the previously described method (Imaizumi *et al.* 1989) with slight modifications. In brief, mice were anaesthetized with ether and killed by decapitation. UB was dissected out and freed from other tissues in Ca^{2+}-free Krebs solution. The tissue was immersed in Ca^{2+}-free Krebs solution for 30–60 min in a test tube at 37°C. Subsequently, the solution was replaced with Ca^{2+}-free Krebs solution containing 0.2–0.3% collagenase (Amano enzyme, Nagoya, Japan). After 10–15 min treatment, the solution was replaced with Ca^{2+}-free and collagenase-free Krebs solution. The tissue was then gently triturated using a glass pipette to isolate cells. At the start of each experiment, a few drops of the cell suspension were placed in a recording chamber. The bath was continuously perfused with Hepes-buffered solution at a flow rate of 5 ml min^{-1}.

Electrical recording and data analysis

Whole-cell voltage clamp was applied to single cells with patch pipettes using a CEZ-2400 (Nihon Kohden, Japan) amplifier. The pipette resistance ranged from 2 to 5 MΩ, when filled with pipette solution. The seal resistance was approximately 30 GΩ. Data were stored and analysed using menu-drive software as previously reported (Imaizumi *et al.* 1996). Membrane currents were digitized using a pulse coding modulator (PCM) recording system (PCM-501ES; Sony, Tokyo, Japan) and stored on video tape. Data on tapes were replayed onto a personal computer using data acquisition software. Data analysis was done on a computer using software (Cell-Soft) developed at the University of Calgary, Canada. Leakage currents at potentials positive to −60 mV were subtracted

on the computer, assuming a linear relationship between current and voltage in the range of −90 mV to −60 mV. All experiments were done at room temperature (23 ± 1°C).

For intracellular recordings, thin strips (3 × 3 mm) of UB were removed from the mucosal layer of a bladder. A strip was pinned to the bottom in a 1 ml chamber, perfused with Hepes-buffered Krebs solution gassed with 95% O_2–5% CO_2 at a rate of 2–4 ml min^{-1} and kept at 36 ± 1°C and pH 7.4. The transmembrane potential was measured with conventional glass microelectrodes, having resistance of 35–50 MΩ, and amplified by a high input impedance amplifier with capacitance neutralization (MEZ-7200, Nihon Kohden, Tokyo, Japan) for monitoring on a dual-beam storage oscilloscope (VC-10, Nihon Kohden). The transmembrane potential was recorded continuously using a pen recorder (FBR-251 A, TOA Electrics, Ltd, Tokyo, Japan). During experimental manoeuvres, Hepes-buffered Krebs solution was used as the external solution.

Measurement of Ca^{2+} signal from single cells

Ca^{2+} images were obtained using a fast laser-scanning confocal microscope (RCM 8000; Nikon, Japan) and ratio3 software (Nikon, Japan) in the same manner as reported previously (Imaizumi *et al.* 1998; Ohi *et al.* 2001). A myocyte was loaded with 100 μM fluo-4 or fluo-5 by diffusion from the patch pipette. Excitation light of 488 nm from an argon ion laser was delivered through a water-immersion objective (Nikon Fluo ×40, 1.15 NA). Emission light of > 515 nm was detected by a photomultiplier. Fluorescence intensity (F) in a selected area was measured as an average from pixels included in the area. It took 33 ms to scan one frame (512 × 512 pixels). Using 1/2 and 1/4 band scan modes, frames that corresponding to areas of 170 × 55 μm or 170 × 27.5 μm were obtained every 16.5 and 8.25 ms, respectively. The resolution of the microscope was approximately 0.4 × 0.3 × 1.2 μm (x, y and z) based on the measurement using fluorescent beads having diameters of 300, 500, 1000 and 1500 nm (sicastar-green F, Nacalai Tesque, Kyoto, Japan). The confocal plane through the cell was usually set, at a position where the width of the cell was largest, 2–3 μm from its lowest point. Recordings were started at 3 min after rupturing the patch membrane to allow sufficient time for fluo-4 to diffuse into the myocyte.

In separate experiments, some measurements of Ca^{2+} signals were also performed using fura-2. Single UBSMs were loaded with 10 μM fura-2 AM in standard Hepes-buffered solution for 20 min at room temperature (23 ± 1°C). Measurements of fura-2 fluorescence were performed with an Argus 50/CA imaging system (Hamamatsu Photonics, Japan). The frequency of image acquisition was constant at one image every 1 s. The intensity of emission fluorescence > 510 nm was measured to the alternate excitation (340 nm and 380 nm). The experiments were carried out at room temperature.

Measurements of contractility from urinary bladder tissue strips

Measurements of contractility from UB tissue strips were carried out as reported previously (Morimura *et al.* 2006). In brief, 8- to 12-week old male mice were anaesthetized with ether and killed by decapitation, and the UB was removed and placed in Ca^{2+}-free Krebs solution. The bladder was then cut open. The detrusor muscle was isolated as small strips (0.8–1.2 mm wide and 5–6 mm long). Each strip was placed in a tissue bath (∼6 ml in volume) containing aerated Krebs solution with 95% O_2 and 5% CO_2 and kept at 37°C. One end of the strip was pinned to the chamber bottom while the other end was connected to a force-displacement transducer for measurement of isometric contractility. Strips were stretched to approximately 1 mN of tension. To apply electrical field stimulation, platinum stimulating electrodes were placed along a tissue in both sides. Electrical field stimulation protocols are shown in the inset of Fig. 4*A*. To suppress the contractile component due to transmitter release from nerve endings in the bladder strips, all experiments using tissue strips were conducted in the presence of the following neurotransmitter antagonists (μM): 1 atropine, 1 phentolamine, 1 propranolol, 1 tetrodotoxin and 10 suramin.

Solution

Standard Krebs solution was made daily and contained (mM): 112 NaCl, 4.7 KCl, 2.2 $CaCl_2$, 1.2 $MgCl_2$ 25 $NaHCO_3$, 1.2 KH_2PO_4, 14 glucose. Ca^{2+}-free Krebs solution was prepared by omitting Ca^{2+} from standard Krebs solution. Ca^{2+}- and Mg^{2+}-free Hanks' solution contained (mM): 137 NaCl, 5.4 KCl, 0.17 Na_2HPO_4, 0.44 KH_2PO_4, 4.2 $NaHCO_3$, 5.6 glucose. Standard and modified Krebs solutions and Ca^{2+}- and Mg^{2+}-free Hanks' solution were aerated with 95% O_2–5% CO_2 to obtain pH 7.4. For measurements of transmembrane potential with conventional glass microelectrodes, Hepes-buffered Krebs solution having the following composition was used as the external solution (mM): 120 NaCl, 4.8 KCl, 1.2 $CaCl_2$, 1.3 $MgSO_4$, 12.6 $NaHCO_3$, 1.2 KH_2PO_4, 5.8 glucose, 10 Hepes and aerated with 95% O_2–5% CO_2 to obtain pH 7.4. For electrical recording from isolated myocytes, Hepes-buffered solution having the following composition was used as the external solution (mM): 137 NaCl, 5.9 KCl, 2.2 $CaCl_2$, 1.2 $MgCl_2$, 14 glucose, 10 Hepes, and pH was adjusted to 7.4 with NaOH. In some experiments, K^+ currents were blocked by use of an external solution, in which 31 mM KCl was replaced by 30 mM tetraethylammonium chloride and 1 mM 4-aminopyridine-HCl.

The standard pipette solution for membrane current recording contained (mM): 140 KCl, 4 $MgCl_2$, 10 Hepes, 5 Na_2ATP, 0.05 EGTA and pH was adjusted to 7.2 with KOH. When recording only Ca^{2+} channel currents, the pipette solution contained (mM): 120 CsCl, 20 tetraethylammonium chloride, 1 $MgCl_2$, 10 Hepes, 5 EGTA, 2 Na_2ATP, and pH was adjusted to 7.2 with CsOH. To measure whole K^+ currents including Ca^{2+} activated K^+ currents, a pipette solution of following composition was used (mM): 140 KCl, 1 $MgCl_2$, 6.1 $CaCl_2$, 10 Hepes, 2 Na_2ATP, 10 EGTA, and the pH of the solution was adjusted to 7.2 with KOH. The pCa of the solution was calculated to be 6.5. When measuring both fluo-4 signals and membrane currents, the pipette solution having the following composition was used (mM): 140 KCl, 1 $MgCl_2$, 10 Hepes, 2 Na_2ATP, 0.1 fluo-4, and pH was adjusted to 7.2 with KOH.

Urination patterns

Female mice of 10–14 weeks old were used in these experiments. After stopping the supply of water for a day, water (1 ml) was supplied to mice by the probe. Mice were then placed in standard cages for 1 h with the bedding replaced by filter paper (Advantec, Japan). Urine spots were photographed under UV light (Meredith *et al.* 2004).

Materials

The sources of pharmacological agents were as follows: $CdCl_2$, tetraethylammonium chloride (TEA), 4-aminopyridine (4-AP), ryanodine, caffeine: Wako Pure Chemical Industries, Osaka, Japan; acetylcholine (ACh), paxilline: Sigma Chemical Co., St Louis, MO, USA; EGTA, Hepes: Dojin, Kumamoto, Japan); fluo-4, fluo-5, fura-2 AM: Molecular Probes, Eugene, OR, USA.

Statistical analysis

Data are expressed as the mean ± S.E.M. in the text. Statistical significance between two or among multiple groups was examined using Student's *t* test or Tukey's test after an *F*-test or one-way ANOVA, respectively. Significance is expressed in the figures by asterisks: $^*P < 0.05$, $^{**}P < 0.01$.

Results

Changes in mRNA expression levels of RyR subtypes in RyR2$^{+/-}$ animals

The mRNA expression levels of RyR1, RyR2 and RyR3 were determined based on real-time PCR in various tissue types of *RyR2*$^{+/+}$ and *RyR2*$^{+/-}$ (Fig. 1, Supplemental Table). As expected, RyR1 mRNA is expressed abundantly in skeletal muscle (diaphragm), but at much lower level in other tissues. There was no difference in RyR1 mRNA expression levels in skeletal muscle between *RyR2*$^{+/+}$ and *RyR2*$^{+/-}$ progeny (Fig. 1*A*). The analysis also confirmed that RyR2 mRNA was expressed predominantly in heart and moderately in SM tissues (Fig. 1*B*). The RyR2 mRNA expression in heart of *RyR2*$^{+/-}$ was not significantly different from that of *RyR2*$^{+/+}$. The RyR2 mRNA expression examined in eight SM tissues was significantly reduced in *RyR2*$^{+/-}$ animals as compared to that in *RyR2*$^{+/+}$, except for the colon and uterus. RyR3 mRNA was expressed at low levels in a wide variety of tissues, but the levels were relatively high in urinary bladder (UB), vas deferens and uterus (Fig. 1*C*). In uterus, RyR3 mRNA expression was comparable to that of RyR2. The difference in RyR3 mRNA expression levels between *RyR2*$^{+/+}$ and *RyR2*$^{+/-}$ was not significant in any of the tissues examined. The decrease in RyR2 mRNA expression in *RyR2*$^{+/-}$ was the most extensive in UB (by 72%) (Fig. 1*D*).

Preliminary study by the Western blotting analysis using anti-RyR antibody, which identifies all three RyR isoforms, suggested that the expression of RyR protein in UB from *RyR2*$^{+/-}$ was substantially lower than that from *RyR2*$^{+/+}$ (Supplemental Fig. 1). Based on these observations, the present study was focused on the difference in functional contribution of RyR to E-C coupling in UBSM from *RyR2*$^{+/-}$ and *RyR2*$^{+/+}$.

Local Ca^{2+} events and activation of membrane currents during depolarization in UBSMCs

Confocal images of local changes in intracellular Ca^{2+} concentration ($[Ca^{2+}]_i$) and membrane currents during depolarization were simultaneously recorded from UBSMCs isolated from *RyR2*$^{+/+}$ and *RyR2*$^{+/-}$. UBSMCs were loaded with 100 μM fluo-4 by diffusion from recording pipettes during whole cell voltage clamp. Myocytes were depolarized from −60 to 0 mV for 50 ms. Figure 2*A* consists of fluorescent images obtained every 8.25 ms from UBSMCs of *RyR2*$^{+/+}$ and *RyR2*$^{+/-}$. In UBSMC from *RyR2*$^{+/+}$, the rise of $[Ca^{2+}]_i$ during depolarization appeared first as local Ca^{2+} elevations (Ca^{2+} hot spots) in well-defined intracellular locations. Subsequently these changes spread to other parts of cell as has been reported previously (Ohi *et al.* 2001; Morimura *et al.* 2006). In the image obtained 26.9 ms after depolarization, Ca^{2+} hot spots were observed in five separate areas in a single confocal plane. This rise of $[Ca^{2+}]_i$ then slowly spread from the spots to the entire intracellar area forming a Ca^{2+} wave even after repolarization (Morimura *et al.* 2006). In contrast, at 26.9 ms, in UBSMC from *RyR2*$^{+/-}$, Ca^{2+} hot spots were detected (4 hot spots in Fig. 2*A*) but less Ca^{2+} wave extension was observed.

Figure 2*B* shows time courses of $[Ca^{2+}]_i$ changes (red and green circles) measured from two Ca^{2+} hot spots,

which are indicated by red and green arrowheads in Fig. 2*A*, respectively. The average signal in the whole cell area is also denoted (blue circles). The rise of local and global $[Ca^{2+}]_i$ in $RyR2^{+/-}$ appeared to be smaller than that in $RyR2^{+/+}$. Figure 2*B* also shows membrane currents (black dots) elicited by depolarization from −60 to 0 mV for 50 ms. The outward current elicited by depolarization in $RyR^{+/-}$ was smaller than that in $RyR^{+/+}$, while the initial inward current appeared to be similar between $RyR^{+/-}$ and $RyR^{+/+}$. The major part of the outward current recorded at 0 mV (by over 80%) was inhibited by addition of 1 μM paxilline or 100 nM iberiotoxin (not shown) (Morimura *et al.* 2006). These findings indicate that BK channel current is responsible for the major part of this outward current as has been reported previously (Imaizumi *et al.* 1998). The cell capacitance of UBSMCs was not different between $RyR2^{+/+}$ (44.4 ± 2.33 pF, $n = 20$) and $RyR2^{+/-}$ (45.5 ± 1.92 pF, $n = 19$; $P > 0.05$).

Figure 2*C* summarizes the $[Ca^{2+}]_i$ results (F/F_0) measured at Ca^{2+} hot spots and in whole cell area in $RyR2^{+/+}$ and $RyR2^{+/-}$ UBSM cells. The $[Ca^{2+}]_i$ rise in hot spots in $RyR2^{+/-}$ was significantly smaller than that in $RyR2^{+/+}$ ($P < 0.01$). The global $[Ca^{2+}]_i$ rise in $RyR2^{+/-}$ was also significantly smaller than that in $RyR2^{+/+}$ ($P < 0.01$). Figure 2*D* denotes summarized results which describe the number of Ca^{2+} hot spots per single confocal image obtained after 18.7 ms depolarization typically shown in Fig. 2*A*. Ca^{2+} hot spots in $RyR2^{+/-}$ was

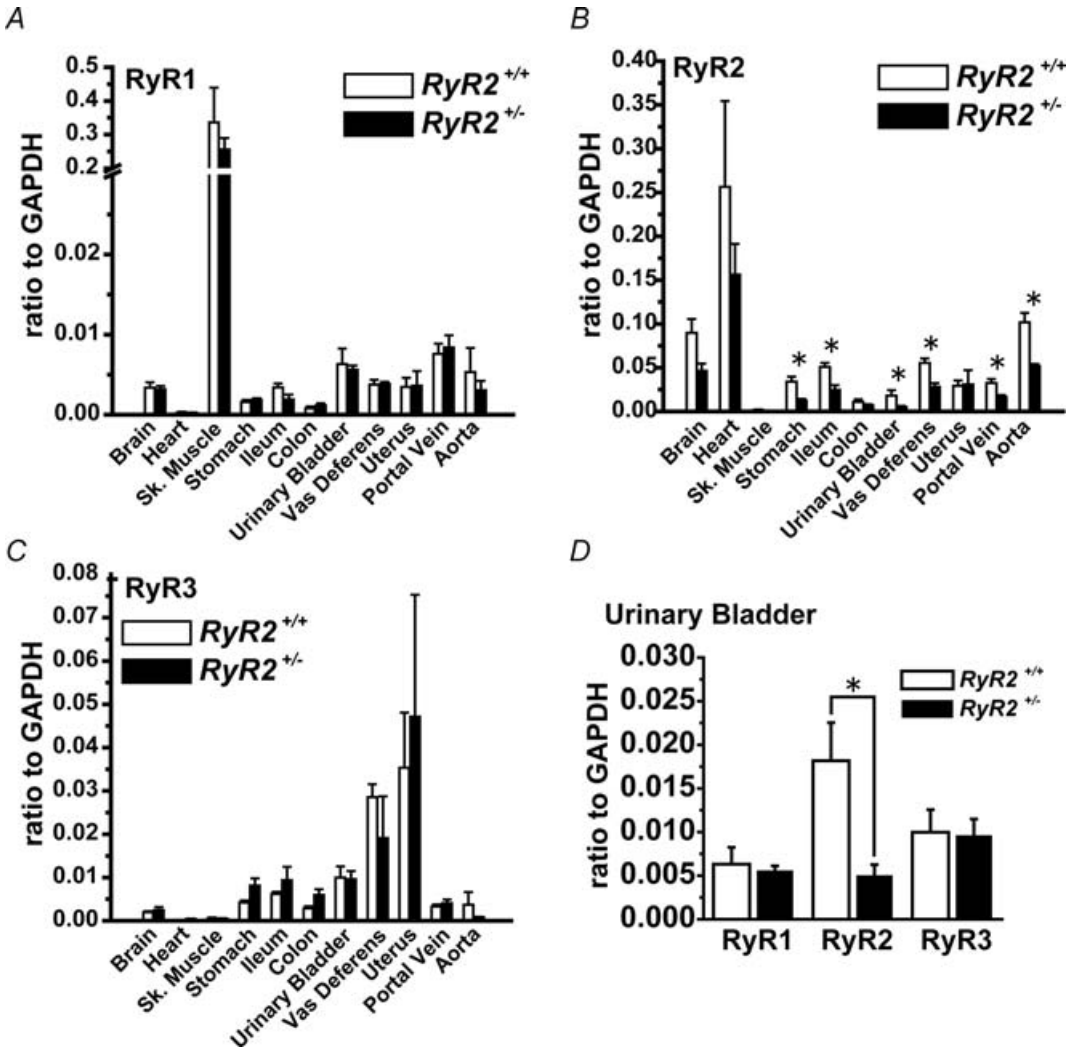

Figure 1. The mRNA expression of RyR subtypes in various tissues from $RyR2^{+/+}$ and $RyR2^{+/-}$
Quantitative analyses for RyR subtypes were performed by real-time PCR. RyR1 (*A*), RyR2 (*B*) and RyR3 (*C*) mRNA expression levels were compared between $RyR2^{+/+}$ and $RyR2^{+/-}$. *A*, $n = 4$, except for portal vein and aorta of $RyR2^{+/-}$ ($n = 3$); *B*, $n = 4$, except for urinary bladder of $RyR2^{+/+}$ ($n = 8$) and portal vein and aorta of $RyR2^{+/-}$ ($n = 3$); *C*, $n = 4$, except for portal vein and aorta of $RyR2^{+/-}$ ($n = 3$). *D*, comparison of mRNA expression levels of RyR1–3 in urinary bladder. $n = 4$, except for RyR2 of $RyR2^{+/+}$. *$P < 0.05$ *versus* $RyR2^{+/+}$.

significantly smaller than that in $RyR2^{+/+}$ ($P < 0.05$). Moreover, the averaged peak amplitude of outward current in $RyR2^{+/-}$ was significantly smaller than that of $RyR2^{+/+}$ ($P < 0.05$) (Fig. 2*E*).

Simultaneous recordings of Ca^{2+} images and voltage-dependent Ca^{2+} (VDCC) currents were also performed in the presence of 30 mM tetraethyammonium (TEA) and 1 mM 4-aminopyridine (4-AP) to block K^+ currents (Supplemental Fig. 2). Cells were depolarized from −60 to 0 mV for 30 ms in the same manner as Fig. 2. Results were roughly the same as those shown in Fig. 2. $[Ca^{2+}]_i$ rises in hot spots (F/F_0: 2.80 ± 0.211, $n = 16$) and whole cell area (2.08 ± 0.307, $n = 5$) in $RyR2^{+/-}$ were significantly smaller than those in $RyR2^{+/+}$, respectively (4.29 ± 0.157, $n = 31$, $P < 0.001$; 3.31 ± 0.370, $n = 6$, $P < 0.05$). The number of Ca^{2+} hot spots in images at 18.7 ms in $RyR2^{+/-}$ (3.2 ± 0.20, $n = 5$) was significantly smaller than that in $RyR2^{+/+}$ (5.0 ± 0.63, $n = 6$, $P < 0.05$). The current density of peak VDCC current at 0 mV was comparable between $RyR2^{+/+}$ (-7.06 ± 0.784, $n = 6$) and $RyR2^{+/-}$ (-6.65 ± 1.28, $n = 5$; $P > 0.05$).

We also measured the density of VDCC currents and BK channel currents in $RyR2^{+/+}$ and $RyR2^{+/-}$ UBSM cells under the conditions where $[Ca^{2+}]_i$ was strongly buffered. In these protocols, myocytes were depolarized for 200 ms from a holding potential of −60 mV to test potentials in 10 mV steps. To measure VDCC currents, outward currents were blocked by Cs^+ in the pipette solution, which also included 5 mM EGTA (see Methods). Figure 3*A* shows the relationship between the current density and test potentials for VDCC. The peak VDCC was measured at +10 mV. Note that there was no difference in the current density between $RyR2^{+/+}$ and $RyR2^{+/-}$ at any potentials examined. The shape of VDCC measured at +10 mV in $RyR2^{+/-}$ was also comparable to that in $RyR2^{+/+}$; the ratio of VDCC current amplitude at the end *versus* that at the peak was 0.642 ± 0.025 ($n = 20$) in $RyR2^{+/+}$ and 0.618 ± 0.019 ($n = 19$, $P > 0.05$) in $RyR2^{+/-}$.

To measure the density of BK channel current, outward currents were recoded under the conditions, where $[Ca^{2+}]_i$ was fixed at pCa 6.5 by Ca^{2+}-EGTA buffer and the Ca^{2+} influx was blocked by 0.1 mM Cd^{2+}. Figure 3*B* shows the outward K^+ currents under these conditions. The *I–V* relationships were obtained before and after BK channel currents were blocked by 1 μM paxilline. Figure 3*B* demonstrates *I–V* relationships of BK channel current density as the current component sensitive to paxilline. There was no difference in the current density between $RyR2^{+/+}$ and $RyR2^{+/-}$ at any potentials examined.

Contribution of RyR2 to contraction

Contractions induced by direct electrical stimulation were measured from UBSM strips of $RyR2^{+/+}$ and $RyR2^{+/-}$ in the presence of various neurotransmitter antagonists. Figure 4*A* shows representative measurement of contractions induced with electrical field stimulation in four separate conditions (the inset table). The amplitude of contraction depended on the stimulation conditions and could be summarized as follows: (1) the contraction resulting from a train of 10 pulses (10 ms in duration) and applied at 200 ms intervals > (2) a train of 10 pulses (3 ms in duration) and 200 ms in interval > (3) a single pulse at 10 ms in duration > (4) a single pulse at 3 ms in duration. Addition of 100 μM ryanodine transiently increased the tone and reduced the amplitude of contraction in both $RyR2^{+/+}$ and $RyR2^{+/-}$. The increased tone returned to the baseline level with time, whereas the contractions by electrical stimulation remained small even after washout of ryanodine (not shown).

When contraction was induced by single 3 ms pulse, the contraction in $RyR2^{+/-}$ was significantly smaller than that in $RyR2^{+/+}$ ($P < 0.01$) (Fig. 4*B*). This contraction was markedly reduced by ryanodine in tissues from $RyR2^{+/+}$, but not changed significantly in $RyR2^{+/-}$. In the presence of ryanodine, the contraction amplitude due to a single 3 ms stimulation was comparable between $RyR2^{+/+}$ and $RyR2^{+/-}$. When the contraction was induced by the train of 10 pulses (10 ms in duration), the amplitude in $RyR2^{+/-}$ was not significantly different from that of $RyR2^{+/+}$ ($P > 0.05$) (Fig. 4*C*). It is also notable that the addition of 100 μM ryanodine did not significantly change the amplitude in both $RyR2^{+/+}$ and $RyR2^{+/-}$ under these conditions.

The sensitivity of these contractions to 100 μM ryanodine is summarized in Fig. 4*D*. Note that the amplitude of contraction following a single 3 ms pulse was significantly decreased by ryanodine in both $RyR2^{+/+}$ and $RyR2^{+/-}$ but the rate of decrease was much smaller in $RyR2^{+/-}$ than in $RyR2^{+/+}$ ($P < 0.01$). In contrast, the contraction induced by the train of 10 pulses (10 ms in duration) was not significantly changed by ryanodine and the results were comparable between $RyR2^{+/+}$ and $RyR2^{+/-}$ ($P > 0.05$).

To compare the maximum contractile responses in $RyR2^{+/+}$ and $RyR2^{+/-}$, 10 μM ACh was applied in each preparation at the beginning of experiment. No significant difference was observed between $RyR2^{+/+}$ (3.1 ± 0.15 mN mg^{-1}, $n = 16$) and $RyR2^{+/-}$ (2.8 ± 0.20 mN mg^{-1}, $n = 13$; $P > 0.05$).

Sensitivity to caffeine

Ca^{2+} release by caffeine from SR through RyR was examined in UBSMCs from $RyR2^{+/-}$ and $RyR2^{+/+}$. Ca^{2+} fluorescence intensity ratios based on fura-2 (F_{340}/F_{380}) were measured in single UBSMCs (Fig. 5*A*). When caffeine was added sequentially at concentrations from 0.3 to

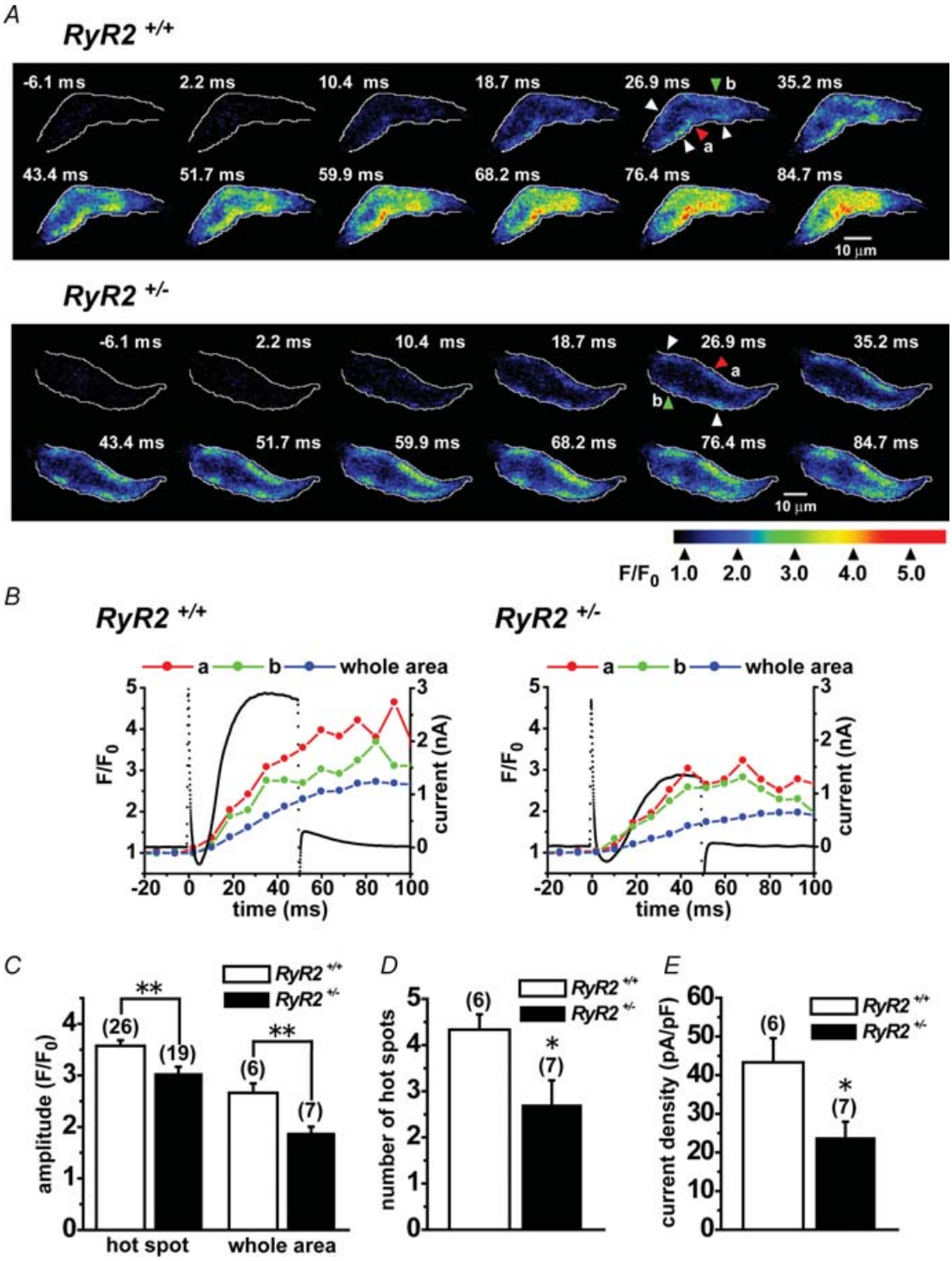

Figure 2. Ca^{2+} hot spots observed following depolarization in UBSM cells from *RyR2*$^{+/+}$ and *RyR2*$^{+/-}$
Membrane currents and Ca^{2+} events were simultaneously monitored in single UBSM cells isolated from *RyR2*$^{+/+}$ and *RyR2*$^{+/-}$ under voltage clamp. Ca^{2+} images were obtained using fluo-4 and laser scanning confocal microscopy. *A*, representative Ca^{2+} images during and following depolarization from −60 to 0 mV for 50 ms in *RyR2*$^{+/+}$ and *RyR2*$^{+/-}$ UBSM cells. Voltage clamp depolarization started at 0 ms. The edge of cells is indicated by the white line. Arrows indicated hot spots. The Ca^{2+} hot spots were identified and measured in the images as follows (Ohi *et al.* 2001). (1) The averaged fluorescence intensity ratio (F/F_0) in a cluster of pixels, which includes neighbouring 4 pixels or more, was larger than 2.0. (2) The F/F_0 in a hot spot was measured as the average at pixels in a circular spot of 1.3 μm in diameter. (3) The area of the hot spot spreads and the F/F_0 in it increased or maintained the high level over 100 ms. *B*, changes in F/F_0 in the small area of hot spots 'a' (red) and 'b' (green) were measured

50 mM, the rise of Ca^{2+} fluorescence intensity due to caffeine was increased in a concentration-dependent manner in both $RyR2^{+/-}$ and $RyR2^{+/+}$. The changes in ratio by caffeine in $RyR2^{+/-}$ were not significantly different from those in $RyR2^{+/+}$ at any concentrations of caffeine examined (Fig. 5*B*). In Fig. 5*C*, these data are normalized to the maximum in each cell and the caffeine concentration eliciting half-maximum rise of the ratio was obtained in each cell as the EC_{50}. The EC_{50} of caffeine in $RyR2^{+/+}$ (2.9 ± 0.43 mM, $n = 18$–22) was significantly lower than that in $RyR2^{+/-}$ (5.2 ± 0.54 mM, $n = 16$–23; $P < 0.01$) (Fig. 5*C*).

Spontaneous transient outward currents and resting membrane potential

Spontaneous transient outward currents (STOCs) were measured under whole-cell voltage clamp in UBSMCs from $RyR2^{+/+}$ and $RyR2^{+/-}$ at holding potentials in the range from −60 to −30 mV at 10 mV step. Figure 6*A* shows representative recordings at −30 mV. Note that the frequency of STOCs with the peak amplitude over 20 pA at −30 mV in $RyR2^{+/-}$ was significantly lower than that in $RyR2^{+/+}$ ($P < 0.05$) (Fig. 6*B*). In contrast, the averaged amplitude of STOCs was not significantly different between $RyR2^{+/+}$ and $RyR2^{+/-}$ at any potentials examined (Fig. 6*C*). The amplitude histogram of STOCs (Fig. 6*D*) indicates that the distribution of STOCs with small amplitude between 20 and 30 pA was significantly larger in $RyR2^{+/-}$ than in $RyR2^{+/+}$ ($P < 0.05$). Integrated STOCs per 1 s from base line at −30 mV in $RyR2^{+/-}$ was significantly smaller than that of $RyR2^{+/+}$ ($P < 0.05$) (Fig. 6*E*).

The resting membrane potentials were measured from tissue preparations using conventional glass microelectrodes in the presence of 1 μM atropine. The resting membrane potential in $RyR2^{+/-}$ (-44.7 ± 0.74 mV, $n = 11$) was slightly but significantly more depolarized than that in $RyR2^{+/+}$ (-46.8 ± 0.68 mV, $n = 10$; $P < 0.05$) (Supplemental Fig. 3). In the presence of 1 μM paxilline, there was no difference in the membrane potentials between $RyR2^{+/+}$ (-41.5 ± 0.90 mV, $n = 11$) and $RyR2^{+/-}$ (-41.9 ± 0.90 mV, $n = 10$; $P > 0.05$). The extent of depolarization by paxilline in $RyR2^{+/-}$ (3.3 ± 0.41 mV, $n = 11$) was significantly smaller than that in $RyR2^{+/+}$ (5.0 ± 0.57 mV, $n = 10$; $P < 0.05$).

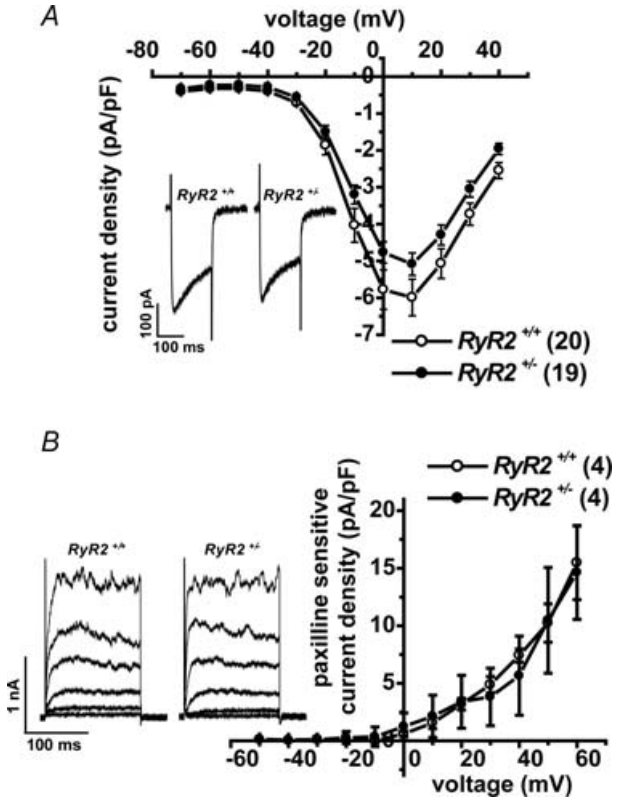

Figure 3. Current density of VDCC currents and BK channel currents in UBSM cells from $RyR2^{+/+}$ and $RyR2^{+/-}$
A, the voltage dependence of VDCC current density was determined as *I–V* relationships. By replacement of K^+ in the pipette filling solution with Cs^+, K^+ currents were suppressed, and VDCC currents were obtained as the 100 μM Cd^{2+} sensitive current component. Intracellular Ca^{2+} was buffered with 5 mM EGTA in the pipette solution (no addition of Ca^{2+}). Cells were depolarized for 150 ms from −60 mV to test potentials by 10 mV step. The average of peak current density in UBSMCs of $RyR2^{+/+}$ and $RyR2^{+/-}$ UBSM cells was plotted against test potentials, to which cells were depolarized from −60 mV ($RyR2^{+/+}$, ○, $n = 20$; $RyR2^{+/-}$, ●, $n = 19$). Note that there was no significant difference in current density between $RyR2^{+/+}$ and $RyR2^{+/-}$ at any potentials examined. Inset shows the current traces at + 10 mV. *B*, the *I–V* relationships for BK currents were obtained under fixed $[Ca^{2+}]_i$. The $[Ca^{2+}]_i$ in the pipette solution was adjusted at pCa 6.5 with 10 mM EGTA and suitable Ca^{2+}. Ca^{2+} influx was blocked by 100 μM Cd^{2+}. Cells were depolarized for 150 ms from −60 to test potentials by 10 mV step. The inset shows outward currents at −40, −20, 0, +20, +40 and +60 mV. BK channel currents were measured as 1 μM paxilline sensitive current component. The relationships between the density of BK current component were plotted against test potentials ($RyR2^{+/+}$, ○, $n = 4$; $RyR2^{+/-}$, ●, $n = 4$). There was no significant difference in current density between $RyR2^{+/+}$ and $RyR2^{+/-}$ at any potentials examined.

from two Ca^{2+} hot spots indicated by red and green arrowheads in *A*, respectively. The data are plotted against time. F_0 was the average fluorescence intensity before depolarization. F/F_0 ratios measured as the average from whole cell area (blue) were also plotted. The black dots show membrane currents under whole cell voltage clamp. *C*, summarized data of $[Ca^{2+}]_i$ increases detected as peak F/F_0 at Ca^{2+} hot spots and in whole cell areas. Data were obtained from experiments shown in *A*. The numerals in parentheses indicate number of cells examined. *D*, number of Ca^{2+} hot spots per cell. The Ca^{2+} hot spots were measured in one confocal plane obtained 18.7 ms after the start of depolarization in the experiments shown in *A*. The numerals in parentheses indicate number of cells examined. *E*, peak amplitude of outward currents activated by depolarization from −60 to 0 mV for 50 ms as shown in *A*. The numerals in parentheses indicate number of cells examined. $*P < 0.05$, $**P < 0.01$ *versus* $RyR2^{+/+}$ in *C*, *D* and *E*.

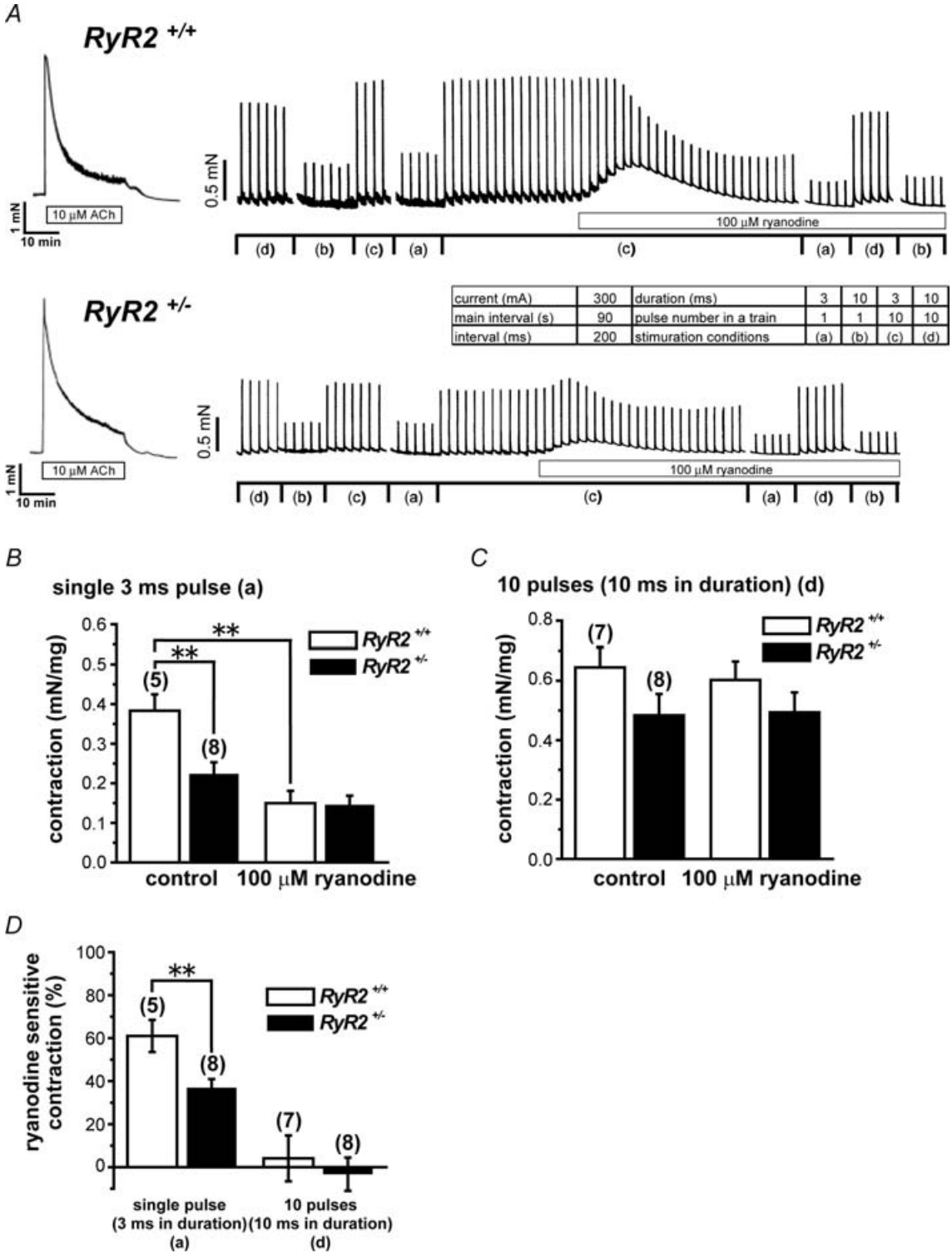

Figure 4. Measurement of contractions and effects of 100 μm ryanodine
A, representative traces of contractions recorded from UBSM strips. Inset shows four sets of conditions, (a)–(d), for electrical stimulation. In the presence of various neurotransmitter antagonists (1 μM atropine, 1 μM phentolamin, 1 μM propranolol, 1 μM TTX, 10 μM suramin), contractions were induced by electrical field stimulation in UBSM strips every 90 s. Changes in contraction magnitude by 100 μM ryanodine were compared between *RyR2*$^{+/+}$ and *RyR2*$^{+/-}$. *B*, summarized data based on contractions evoked by single 3 ms pulse corresponding to the stimulation condition (a) in the inset of *A*, before (control: left two columns) and after the addition of 100 μM ryanodine (right two columns). Open and filled columns indicate *RyR2*$^{+/+}$ and *RyR2*$^{+/-}$, respectively. Data were collected from

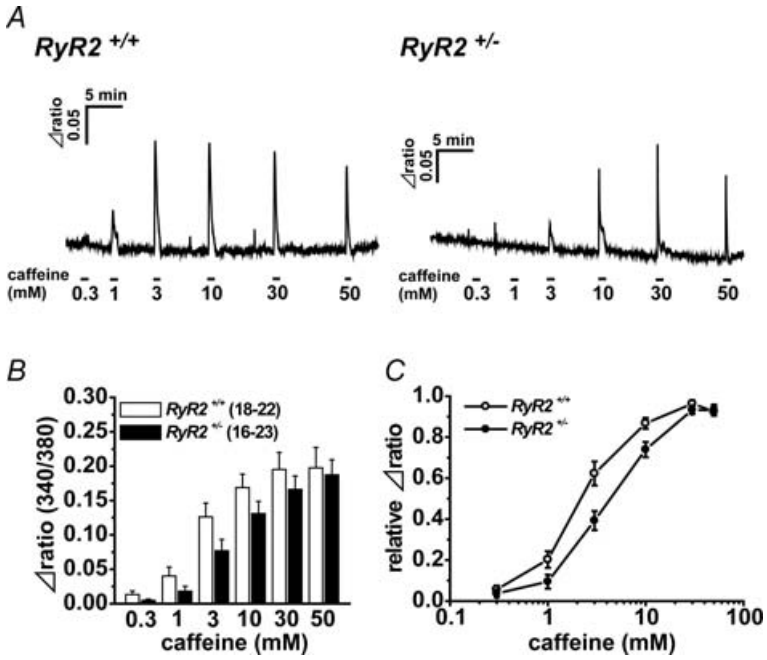

Figure 5. Difference in caffeine sensitivity between *RyR2*$^{+/+}$ and *RyR2*$^{+/-}$ UBSM cells
The rise of $[Ca^{2+}]_i$ elevated by caffeine in UBSMCs was compared between *RyR2*$^{+/+}$ and *RyR2*$^{+/-}$. UBSM cells were loaded by fura-2 AM, and Ca^{2+} fluorescence intensity ratio (F_{340}/F_{380}) was measured. *A*, caffeine was added sequentially at concentrations from 0.3 to 50 mM. *B*, summarized data showing the rise of fura-2 ratio (Δratio) activated at each concentration of caffeine. *C*, the relationships between concentrations of caffeine and the relative Δratio. The data shown in *B* were replotted by taking the maximum Δratio as unity in each cell. The numerals in parentheses indicate the number of cell examined.

mRNA expression of molecules regulating Ca^{2+} mobilization in subcellular microdomain

The mRNA expression levels of molecules which were related to Ca^{2+} mobilization in SMCs were compared quantitatively in UB from *RyR2*$^{+/+}$ and *RyR2*$^{+/-}$. This analysis included: junctophilin type 2 (JP2), VDCC (α1c, β2, β3), Ca^{2+} activated K^+ channel (BK, SK2, SK4), SR/ER Ca^{2+}-ATPase (SERCA2), IP_3 receptor type1 (IP_3R1), FK506 binding protein (FKBP1a, 1b) and Sorcin.

JP is a protein that is a component of the junctional complex between the plasma membrane and ER/SR (Nishi *et al.* 2000; Takeshima *et al.* 2000; Moriguchi *et al.* 2006). In the present study, JP2 mRNA expression level in UB was much larger than that in heart. JP2 expression level in brain was negligible. JP2 mRNA expression levels in heart and UB were not different between *RyR2*$^{+/+}$ and *RyR2*$^{+/-}$ ($P > 0.05$) (Fig. 7*A*). Based on our analyses of mRNA expression of VDCC subunits, α1c, β2 and β3 subunits in UB, significant difference between *RyR2*$^{+/+}$ and *RyR2*$^{+/-}$ was only observed in β3 subunit. The difference was relatively small ($P < 0.05$) (Fig. 7*B*). The mRNA expression of Ca^{2+} activated K^+ channels (BK, SK2, SK4/IK), SERCA2 and IP_3R mRNA was not significantly different between *RyR2*$^{+/+}$ and *RyR2*$^{+/-}$ UB (Fig. 7*C–E*). FKBP1a (FKBP 12) mRNA expression level in *RyR2*$^{+/-}$ UB was smaller than that in *RyR2*$^{+/+}$ ($P < 0.05$), but the difference was small (Fig. 7*F*). There was no significant difference of FKBP1b (FKBP12.6) mRNA expression between *RyR*$^{+/+}$ and *RyR2*$^{+/-}$. Sorcin is a molecular component, which may modulates Ca^{2+} release through RyR2 in cardiac myocytes and SM as well (Farrell *et al.* 2003). The expression of sorcin mRNA was not significantly different between *RyR2*$^{+/+}$ and *RyR2*$^{+/-}$ (Fig. 7*G*).

Urination patterns in *RyR2*$^{+/+}$ and *RyR2*$^{+/-}$

The possibility that RyR2 deficiency may affect urination activity was examined in *RyR2*$^{+/-}$ in comparison with *RyR2*$^{+/+}$. Urination patterns of freely moving female mice for 1 h after 1 ml water intake were recorded as urine spots on the filter paper (Fig. 8*A*). The averaged area of urine spots from *RyR2*$^{+/-}$ was significantly smaller than that from *RyR2*$^{+/+}$. In contrast, the number of spots of *RyR2*$^{+/-}$ was significantly larger than that of *RyR2*$^{+/+}$. The total area of spots was comparable between them. These results indicate that smaller volume of urine was excreted more frequently from *RyR2*$^{+/-}$ than in *RyR2*$^{+/+}$, while the total urine volume was comparable.

experiments typically shown in *A*. *C*, summarized data based on contractions evoked by the train of 10 pulses (10 ms in duration) corresponding to (d), before (control) and after the addition of 100 μM ryanodine. *D*, summarized data based on the sensitivity of contraction to 100 μM ryanodine. The component of contraction susceptible to ryanodine is shown as a percentage of the contraction before ryanodine application. In *B–C*, the developed force has been normalized to the tissue weight in each preparation (mN mg^{-1}). In *B–D*, the numerals in parentheses indicate number of preparations examined. $^*P < 0.05$, $^{**}P < 0.01$ *versus* *RyR2*$^{+/+}$ or control.

Discussion

Our results demonstrate that RyR2 deficiency in UBSMCs results in a markedly reduced contribution of CICR to E-C coupling in this tissue. In addition, a reduced contribution of BK channel current to the resting membrane potential was observed, presumably due to the reduction of Ca^{2+} spark frequency and related decrease in transient outward current. In combination, these results provide direct evidence for an obligatory role of RyR2 as an essential molecular component of CICR in E-C coupling and also as one of the key regulators of resting membrane potential in SMs.

Evaluation of *RyR2*$^{+/-}$ UBSM is a tool to analyse the physiological roles of RyR2 in SMs

Because RyR2 homozygous KO mice (*RyR2*$^{-/-}$) die at approximately embryonic day 10 as a consequence of cardiac arrest (Takeshima *et al.* 1998), it is difficult to study physiological roles of RyR2 in E-C coupling in SMs in these animals. Another plausible approach involves the application of siRNA directed against RyR2 to cultured SMC. However, it has been reported that RyR2 expression levels in myocytes changes markedly during primary culture (Park *et al.* 1998). In addition, these cultured SMCs may not be suitable for measurement of contraction, which is essential for evaluating E-C coupling.

In the present study, the marked decrease in RyR2 mRNA expression and also RyR protein expression in UB from *RyR2*$^{+/-}$ provide strong motivation to attempting to identify the underlying molecule mechanism. The results obtained by evaluating RyR functions by measuring Ca^{2+} hot spots, STOCs, the sensitivity to caffeine and twitch contraction induced by direct electrical stimulation, all suggest a significant reduction of RyR function. In contrast, mRNA analyses suggest that the expression

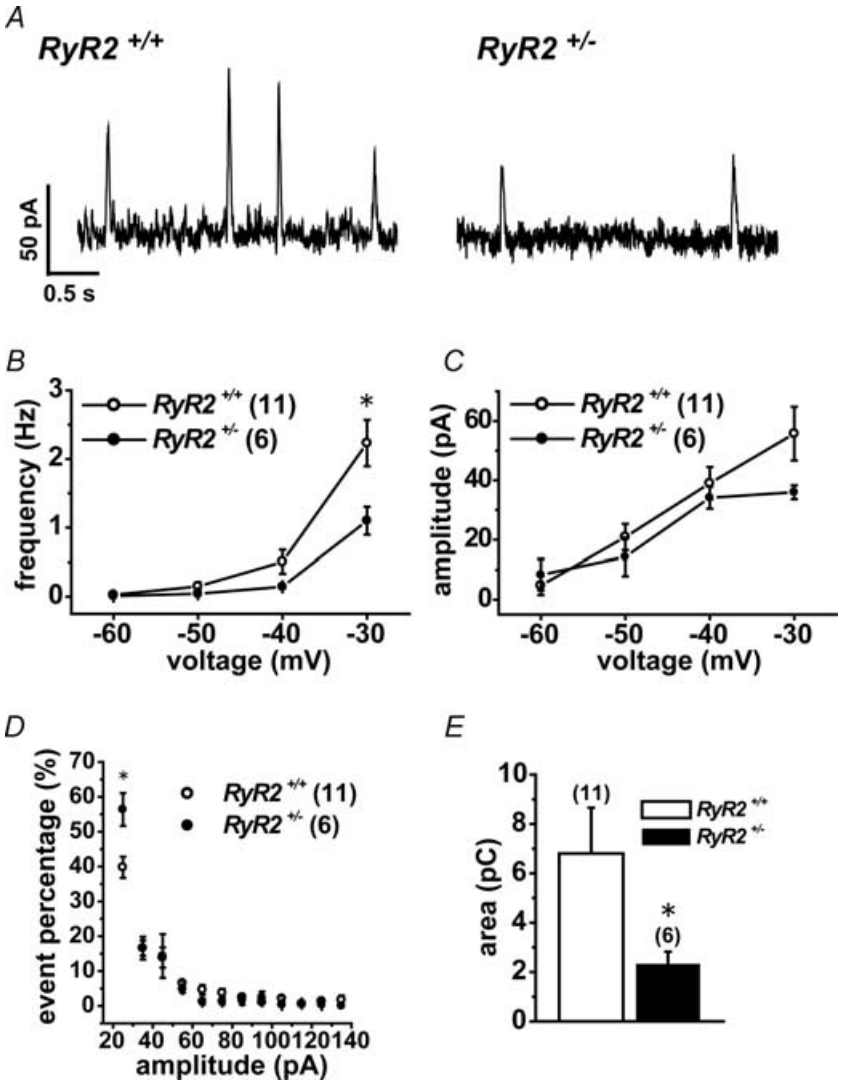

Figure 6. Spontaneous transient outward currents (STOCs) are reduced in UBSM cells of *RyR2*$^{+/-}$
STOCs in UBSMCs from *RyR2*$^{+/+}$ and *RyR2*$^{+/-}$ were measured at holding potentials from −60 to −30 mV at 10 mV step under whole-cell patch clamp. *A*, representative recordings of STOCs at −30 mV in *RyR2*$^{+/+}$ and *RyR2*$^{+/-}$ UBSMCs. *B* and *C*, summarized data of frequency (*B*) and amplitude of STOCs (*C*) at −30 mV in UBSMCs from *RyR2*$^{+/+}$ (○) and *RyR2*$^{+/-}$ (●). *D*, distribution histogram of STOC events against the amplitude in each 10 pA bins over 20 pA. Original data were obtained at a holding potential of −30 mV in UBSMCs from *RyR2*$^{+/+}$ (○) and *RyR2*$^{+/-}$ (●). *E*, charge displacement due to STOCs at a holding potential of −30 mV. *B–E*, numerals in parentheses indicate the number of cells examined. $^*P < 0.05$ *versus* *RyR2*$^{+/+}$.

of molecules known to be essential for local Ca^{2+} regulation, such as L-type VDCC α1C and β2 subunits, BK channel α and β1 subunits, SK2, SK4, SERCA2, IP3R1, FKBP12.6 (FKBP1b), sorcin and junctophilin2 (JP2), was not changed in UB of $RyR2^{+/-}$ in comparison with $RyR2^{+/+}$. FKBP12 (FKBP1a) and VDCC β3 subunits were slightly but significantly reduced. Among four types of JPs, which are component proteins of the junctional complexes between the plasma membrane and ER/SR, JP2 is expressed preferentially in cardiac muscle, smooth muscle and brain (Takeshima *et al.* 2000; Nishi *et al.* 2000). Specifically our finding that JP2 is abundantly expressed in UBSM suggests the existence of 'tight coupling' between RyR and VDCC in mouse UBSMC regardless of $RyR2^{+/-}$ and $RyR2^{+/+}$. Importantly, neither RyR1 nor RyR3 mRNA expression levels were changed in $RyR2^{+/-}$ UB. The PCR primer designed for RyR3 in this study did not distinguish RyR3 splice variants which have been identified recently (Jiang *et al.* 2003; Dabertrand *et al.* 2006). Taken together, our results suggested that RyR2 is selectively and markedly reduced in UB of $RyR2^{+/-}$. This finding provide an important opportunity: UBSMC from $RyR2^{+/-}$ is considered to be an excellent tool to analyse the physiological roles of RyR2 in SMs.

Significant contribution of RyR2 to CICR and E-C coupling in UBSM

There is some controversy about the extent to which CICR contributes to E-C coupling in electrically active SMs. Phenomena corresponding to CICR have been demonstrated in UBSMC of the guinea-pig (Ganitkevich & Isenberg, 1992). Subsequently, however, it has been reported that CICR does not contribute to the SM E-C coupling in portal vein (Kamishima & McCarron, 1996). Another study also concluded that there is only a very limited contribution of CICR to E-C coupling in UB tissue preparations of the guinea-pig (Herrera *et al.* 2000). At present, the function of Ca^{2+} release through RyR in UBSMCs of the guinea-pig has been suggested to be the activation of BK channels but not the contractile system. Kotlikoff and colleagues have proposed 'loose coupling' between VDCC in plasmalemma and RyR in SR for CICR in rabbit UBSMCs (Collier *et al.* 2000; Kotlikoff, 2003). We have recently shown that CICR in UBSMC of the mouse is almost completely blocked by ryanodine and that CICR is essential for E-C coupling triggered by a single action potential (Morimura *et al.* 2006). CICR occurs in two steps during E-C coupling, which is triggered by an action potential; Ca^{2+} influx during an action potential increases

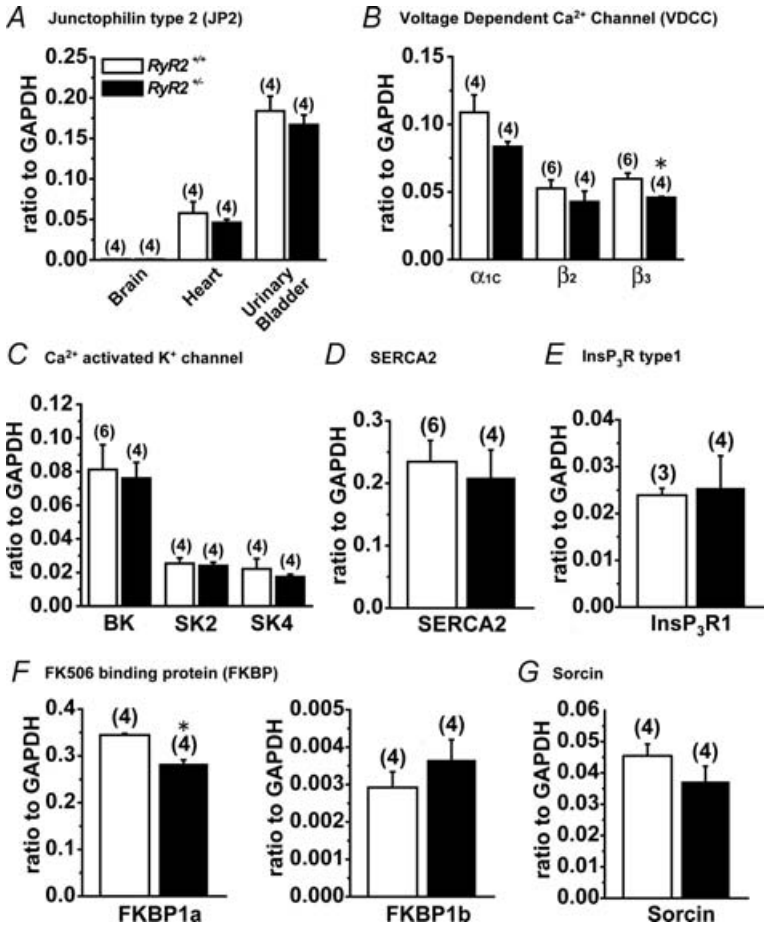

Figure 7. The mRNA expression of molecules related to the regulation of Ca^{2+} mobilization in subcellular microdomains
Quantitative analyses of mRNA expression of several molecules were performed using real-time PCR. *A*, the mRNA expression of junctophilin type 2 (JP2) ($n = 4$). *B*, the mRNA expression of voltage-dependent Ca^{2+} channel (VDCC) α1c, β2 and β3 subunits in UB. $n = 4$, except for β2 and β3 of $RyR2^{+/+}$ ($n = 6$). *C*, the mRNA expression of Ca^{2+} activated K^+ channel subtypes (BK, SK2 and SK4) in UB. $n = 4$, except for BK in $RyR2^{+/+}$ ($n = 6$). *D*, the mRNA expression of Ca^{2+} pump on SR membrane, SERCA2. $n = 4$ and 8 for $RyR2^{+/+}$ and $RyR2^{+/-}$, respectively. *E*, the mRNA expression of $InsP_3$ receptor. $n = 3$ and 4 for $RyR2^{+/+}$ and $RyR2^{+/-}$, respectively. *F* and *G*, the mRNA expression of FK506 binding protein (FKBP1a, 1b) and sorcin in UB, respectively. $n = 4$ for each. *B* and *F*, $^*P < 0.05$ *versus* $RyR2^{+/+}$.

$[Ca^{2+}]_i$ significantly, and this initiates CICR in discrete hot spot sites via functional coupling between VDCCs and ryanodine receptors (Ohi *et al.* 2001). In the second step, which also involves Ca^{2+} release, Ca^{2+} waves slowly spread to other Ca^{2+} store sites in mouse UB; the Ca^{2+} source for twitch contraction induced by an action potential is mainly attributable to CICR following Ca^{2+} influx through VDCC. We acknowledge the possibility that there might be species difference between mouse and guinea-pig/rabbit. The contribution of CICR *versus* that of Ca^{2+} influx as the Ca^{2+} source for contraction in E-C coupling may be larger in mouse UB.

In the present study, both the number of Ca^{2+} hot spots and the increase in $[Ca^{2+}]_i$ in the spots in the early stage of depolarization (< 20 ms) were significantly smaller in UBSMCs of $RyR2^{+/-}$ than in those of $RyR2^{+/+}$.

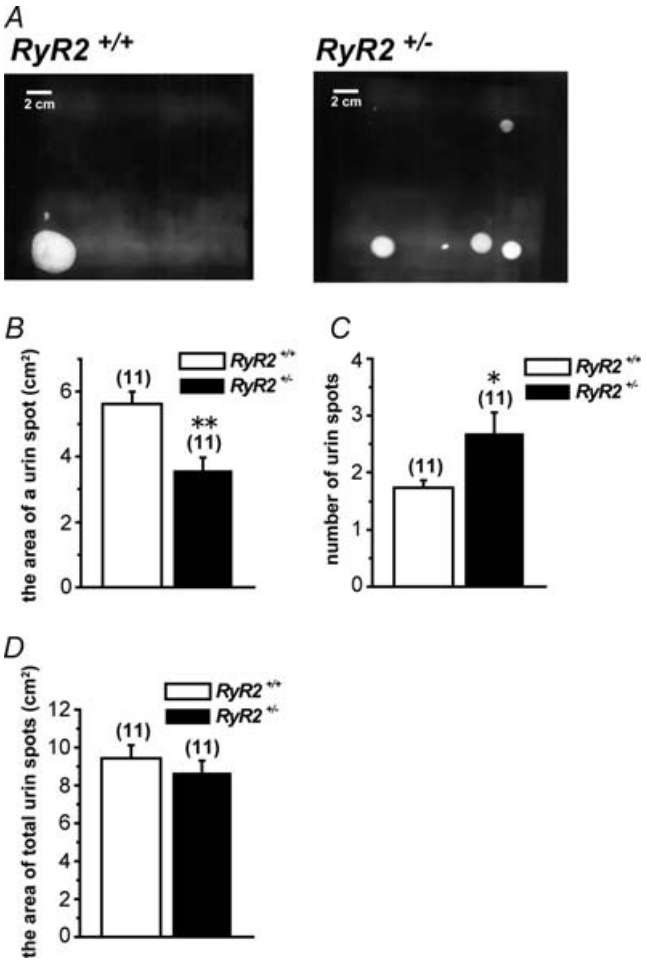

Figure 8. Urinary bladder activity of $RyR2^{+/+}$ and $RyR2^{+/-}$
A, representative urination pattern of freely moving female mice visualized on filter papers under UV light from $RyR2^{+/+}$ and $RyR2^{+/-}$. *B*, average area of a urine spot quantified from filter paper. *C*, average number of urine spots quantified from filter paper. *D*, average area of total urine spots quantified from filter paper. *B–D*, numerals in parentheses indicate the number of animals. $^*P < 0.05$, $^{**}P < 0.01$ *versus* $RyR2^{+/+}$.

Correspondingly, the activation of BK channel current under these conditions was also smaller in $RyR2^{+/-}$ than $RyR2^{+/+}$. Although the deletion of RyR1 results in the decrease in VDCC activity in skeletal muscle (Fleig *et al.* 1996), the density of VDCC was not changed in $RyR^{2+/-}$ in the present study. The density of BK channel current was also not changed in $RyR2^{+/-}$ UBSMCs, in which $[Ca^{2+}]_i$ was fixed at pCa 6.5 (not shown). Therefore, the smaller activation of BK channel current upon depolarization in UBSC from $RyR2^{+/-}$ than that from $RyR^{+/+}$ is presumably due to the decreased function of Ca^{2+} hot spots in $RyR2^{+/-}$ UBSMCs.

The twitch contractions induced by single 3 ms stimulation in UB tissue segments of $RyR2^{+/-}$ were significantly smaller than those of $RyR2^{+/+}$. The decrease in amplitude of these twitch contractions by 100 μM ryanodine was over 60% in $RyR2^{+/+}$ but only 37% in $RyR2^{+/-}$, indicating that the contribution of CICR via RyR2 to the contraction is significantly smaller in $RyR2^{+/-}$. The results for twitch contractions induced by train stimulation (10 pulse 10 ms in duration) were not significantly different between $RyR2^{+/-}$ and $RyR2^{+/+}$. In addition, this pattern of response was not affected by ryanodine, indicating that Ca^{2+} influx through VDCC is the predominant sources of Ca^{2+} for contraction under the severe stimulation conditions. Taken together, these findings strongly suggest that RyR2 is the essential and central molecule responsible for CICR elicited by a single action potential in mouse UBSMCs.

Regulation of resting membrane potential by RyR2

STOCs were first identified in 1986 in intestinal SMs (Benham & Bolton, 1986). They have been shown to be due to a burst of openings of BK channels following spontaneous local Ca^{2+} release (Bolton & Imaizumi, 1996), which has been identified as Ca^{2+} sparks (Nelson *et al.* 1995; Laporte *et al.* 2004). The relationship between Ca^{2+} sparks and the regulation of resting membrane potential by BK channel activity has been well studied in arterial SMs (Knot *et al.* 1998; Imaizumi *et al.* 1999; Jaggar *et al.* 2000) and also in UBSMCs of the guinea-pig (Ohi *et al.* 2001). A well defined functional organization between three molecular components, RyR, BK channels and VDCC, in subcellular microdomains has been suggested; a spontaneous Ca^{2+} spark in the superficial area activates 10–100 BK channels and induces membrane hyperpolarization, which reduces Ca^{2+} channel activity and causes relaxation (Pérez *et al.* 1999; ZhuGe *et al.* 1999; Fürstenau *et al.* 2000). Several lines of evidence have supported this hypothesis. The decreased activity of BK channels following BKβ1 subunit deletion causes arterial hypertension due to a slightly depolarized resting membrane potential and results in increased activity of

VDCC in arterial SMCs (Plüger *et al.* 2000). Bladder instability reported in BKα subunit KO mice may be due to this mechanism (Meredith *et al.* 2004). In this study, it is shown directly that the deficiency of RyR2 resulted in the decrease in STOC frequency and integrated STOCs in *RyR2*$^{+/-}$ UBSMCs in comparison with those in *RyR2*$^{+/+}$. Correspondingly, we found more depolarized resting membrane potential and smaller depolarization by paxiline in UBSM of *RyR2*$^{+/-}$ than those in *RyR2*$^{+/-}$. These results provide further support for the hypothesis that RyR2 is responsible also for the regulation of resting BK channel activity in UBSMCs. Based on this combination of findings, we conclude that spontaneous Ca^{2+} release through RyR2 in junctional SR as Ca^{2+} sparks activates BK channels in the junction and regulates resting membrane potential.

Contribution of RyR2 *versus* RyR3 in UBSMCs

In canine cardiac Purkinje fibre myocytes, in which the T-tubule system is not well developed, substantial functional roles of RyR3, as well as RyR2, have been reported in the generation of Ca^{2+} sparks and Ca^{2+} wavelets (Stuyvers *et al.* 2005). In contrast, detailed information about the functional significance of RyR3 in SMs is limited. The functional roles of RyR2 *versus* RyR3, which is also expressed in UBSM, for Ca^{2+} spark generation has been shown indirectly using RyR3 homozygous KO mice and also FKBP12.6 homozygous KO mice (Ji *et al.* 2005). Since FKBP12.6 selectively interacts with RyR2 and reduces its activity (Marx *et al.* 2001), the increase in Ca^{2+} spark frequency and Ca^{2+} wave speed in FKBP12.6$^{-/-}$ UB is thought to be due to the enhanced activity of RyR2 by FKBP12.6 deficiency (Ji *et al.* 2005). On the other hand, Ca^{2+} sparks and Ca^{2+} waves in UB of RyR3$^{-/-}$ were very similar to those in RyR3$^{+/+}$ UB. Therefore, it has been suggested that RyR3 may not play a significant role in the generation of Ca^{2+} sparks in UBSM. In contrast, an increased frequency of Ca^{2+} sparks has been reported in cerebral artery SMC of RyR3 null mice (Löhn *et al.* 2001). Moreover, novel alternative splice variants of RyR3 have been isolated from SMs (Chen *et al.* 1997; Jiang *et al.* 2003; Dabertrand *et al.* 2006). It has been suggested recently that an alternative splice valiant of RyR3, which works as dominant negative, is predominantly expressed in SM tissues, particularly in uterus (Dabertrand *et al.* 2006). More importantly, RyR3 including the dominant negative type can form a heterotetramer with RyR2 (Jiang *et al.* 2003). It is somewhat puzzling that the dominant negative type variant of RyR3 appears to be extensively expressed even in mouse UB (Dabertrand *et al.* 2006). This finding is not consistent with the lack of changes in Ca^{2+} sparks in RyR3$^{-/-}$ UBSMCs (Ji *et al.* 2003). If the dominant negative splice variant of RyR3 is significantly expressed in mouse UBSMCs as reported, then the functional changes in *RyR2*$^{+/-}$ UBSMCs reported here may possibly be due to both the deficiency of RyR2 *per se* and the increased ratio of dominant negative RyR3 *versus* RyR2. In the present study, however, we show that the maximum rise of caffeine-induced $[Ca^{2+}]_i$ in UBSMCs of *RyR2*$^{+/-}$ is comparable to that in *RyR2*$^{+/+}$, while the sensitivity to caffeine was slightly but significantly reduced in *RyR2*$^{+/-}$. This set of results is not completely consistent with the assumption that the dominant negative splice variant of RyR3 functions in a dominant negative fashion in UBSMCs of *RyR2*$^{+/-}$, since this variant is insensitive to caffeine (Jiang *et al.* 2003; Dabertrand *et al.* 2006).

Potential roles of RyR2 in the regulation of urinary bladder activity

It is notable that the frequency of urination and the volume per voiding were significantly increased and reduced, respectively, in *RyR2*$^{+/-}$ in comparison with those in *RyR2*$^{+/+}$. Interestingly, it has been reported that a model of detrusor instability following outlet obstruction results in down-regulation of RyR expression (Jiang *et al.* 2005). A line of evidence supporting the functional significance of BK channels in the regulation of urination activity has been greatly accumulated (Christ & Hodges, 2006). It has been shown that mice genetically lacking the BK channel α subunit demonstrate a marked increase in urination frequency corresponding to an overactive bladder (Meredith *et al.* 2004). The deficiency of negative feedback mechanism for the control of $[Ca^{2+}]_i$, in which the activation of BK channels plays the central role, is considered to be responsible for the enhanced contractility of bladder smooth muscle in BK channel KO mice. In this respect, both the decreased STOC frequency and the depolarized resulting membrane in UBSMCs from *RyR2*$^{+/-}$ fit with the theory of a central role of BK channels in the regulatory mechanism of bladder function. If it is the case, RyR2 deficiency may result in an overactive bladder. In contrast, the contraction induced by direct electrical stimulation was rather reduced in UB of *RyR2*$^{+/-}$, when the stimulation conditions were moderate. Therefore, it cannot be concluded whether the changes in urination pattern in *RyR2*$^{+/-}$ is due to over-contractility mediated by the reduced activity of BK channels or is simply due to a smaller contribution of CICR to the contraction for voiding. Alternatively, it cannot be ruled out that RyR2 deficiency may result in lower nervous activity to trigger the voiding.

Conclusion

Our findings demonstrate that a down-regulation of RyR2 in UBSMCs can reduce both the contribution

of spontaneous Ca^{2+} release through RyR2 to resting membrane potential and the essential signalling involved in CICR due to depolarization. Thus, RyR2 plays an essential role in CICR for the regulation of E-C coupling induced by an action potential and also in the regulation of resting membrane potential, presumably via the modulation of Ca^{2+} dependent K^+ channel activity in UBSM. It became clear in this study that RyR2 as well as the BK channel (Christ & Hodges, 2006) has a pivotal role in the control of urinary bladder activity. The broader physiological questions related to the influence of RyR2 deficiency in bladder function in *RyR2*$^{+/-}$ and the physiological roles of RyR3 in UBSM remain to be defined and determined.

References

Benham CD & Bolton TB (1986). Spontaneous transient outward currents in single visceral and vascular smooth muscle cells of the rabbit. *J Physiol* **381**, 385–406.

Bolton TB & Imaizumi Y (1996). Spontaneous transient outward currents in smooth muscle cells. *Cell Calcium* **20**, 141–152.

Chambers P, Neal DE & Gillespie JI (1999). Ryanodine receptors in human bladder smooth muscle. *Exp Physiol* **84**, 41–46.

Chen SR, Li X, Ebisawa K & Zhang L (1997). Functional characterization of the recombinant type 3 Ca^{2+} release channel (ryanodine receptor) expressed in HEK293 cells. *J Biol Chem* **272**, 24234–24246.

Christ GJ & Hodges S (2006). Molecular mechanisms of detrusor and corporal myocyte contraction: identifying targets of pharmacotherapy of bladder and erectile dysfunction. *Br J Pharmacol* **147**, S41–S55.

Collier ML, Ji G, Wang YX & Kotlikoff MI (2000). Calcium-induced calcium release in smooth muscle: loose coupling between the action potential and calcium release. *J Gen Physiol* **115**, 653–662.

Dabertrand F, Morel JL, Sorrentino V, Mironneau J, Mironneau C & Macrez N (2006). Modulation of calcium signalling by dominant negative splice variant of ryanodine receptor subtype 3 in native smooth muscle cells. *Cell Calcium* **40**, 11–21.

Fabiato A (1983). Calcium-induced release of calcium from the cardiac sarcoplasmic reticulum. *Am J Physiol Cell Physiol* **245**, C1–C14.

Fabiato A (1985). Simulated calcium current can both cause calcium loading in and trigger calcium release from the sarcoplasmic reticulum of a skinned canine cardiac Purkinje cell. *J Gen Physiol* **85**, 291–320.

Farrell EF, Antaramian A, Rueda A, Gomez AM & Valdivia HH (2003). Sorcin inhibits calcium release and modulates excitation-contraction coupling in the heart. *J Biol Chem* **278**, 34660–34666.

Fleig A, Takeshima H & Penner R (1996). Absence of Ca^{2+} current facilitation in skeletal muscle of transgenic mice lacking the type 1 ryanodine receptor. *J Physiol* **496**, 339–345.

Fürstenau M, Löhn M, Ried C, Luft FC, Haller H & Gollasch M (2000). Calcium sparks in human coronary artery smooth muscle cells resolved by confocal imaging. *J Hypertens* **18**, 1215–1222.

Ganitkevich VY & Isenberg G (1992). Contribution of Ca^{2+}-induced Ca^{2+} release to the $[Ca^{2+}]_i$ transients in myocytes from guinea-pig urinary bladder. *J Physiol* **458**, 119–137.

Giannini G, Clementi E, Ceci R, Marziali G & Sorrentino V (1992). Expression of a ryanodine receptor-Ca^{2+} channel that is regulated by TGF-β. *Science* **257**, 91–94.

Hakamata Y, Nakai J, Takeshima H & Imoto K (1992). Primary structure and distribution of a novel ryanodine receptor/calcium release channel from rabbit brain. *FEBS Lett* **312**, 229–235.

Hashitani H & Brading AF (2003). Ionic basis for the regulation of spontaneous excitation in detrusor smooth muscle cells of the guinea-pig urinary bladder. *Br J Pharmacol* **140**, 159–169.

Hashitani H, Bramich NJ & Hirst GD (2000). Mechanisms of excitatory neuromuscular transmission in the guinea-pig urinary bladder. *J Physiol* **524**, 565–579.

Herrera GM, Heppner TJ & Nelson MT (2000). Regulation of urinary bladder smooth muscle contractions by ryanodine receptors and BK and SK channels. *Am J Physiol Regul Integr Comp Physiol* **279**, R60–R68.

Iino M (1989). Calcium-induced calcium release mechanism in guinea pig taenia caeci. *J Gen Physiol* **94**, 363–383.

Imaizumi Y, Henmi S, Uyama Y, Atsuki K, Torii Y, Ohizumi Y & Watanabe M (1996). Characteristics of Ca^{2+} release for activation of K^+ current and contractile system in some smooth muscles. *Am J Physiol Cell Physiol* **271**, C772–C782.

Imaizumi Y, Muraki K & Watanabe M (1989). Ionic currents in single smooth muscle cells from the ureter of the guinea-pig. *J Physiol* **411**, 131–159.

Imaizumi Y, Ohi Y, Yamamura H, Ohya S, Muraki K & Watanabe M (1999). Ca^{2+} spark as a regulator of ion channel activity. *Jpn J Pharmacol* **80**, 1–8.

Imaizumi Y, Torii Y, Ohi Y, Nagano N, Atsuki K, Yamamura H, Muraki K, Watanabe M & Bolton TB (1998). Ca^{2+} images and K^+ current during depolarization in smooth muscle cells of the guinea-pig vas deferens and urinary bladder. *J Physiol* **510**, 705–719.

Jaggar JH, Porter VA, Lederer WJ & Nelson MT (2000). Calcium sparks in smooth muscle. *Am J Physiol Cell Physiol* **278**, C235–C256.

Ji G, Feldman ME, Greene KS, Sorrentino V, Xin HB & Kotlikoff MI (2004). RYR2 proteins contribute to the formation of Ca^{2+} sparks in smooth muscle. *J Gen Physiol* **123**, 377–386.

Jiang HH, Song B, Lu GS, Wen QJ & Jin XY (2005). Loss of ryanodine receptor calcium-release channel expression associated with overactive urinary bladder smooth muscle contractions in a detrusor instability model. *BJU Int* **96**, 428–433.

Jiang D, Xiao B, Li X & Chen SR (2003). Smooth muscle tissues express a major dominant negative splice variant of the type 3 Ca^{2+} release channel (ryanodine receptor). *J Biol Chem* **278**, 4763–4769.

Kamishima T & McCarron JG (1996). Depolarization-evoked increases in cytosolic calcium concentration in isolated smooth muscle cells of rat portal vein. *J Physiol* **492**, 61–74.

Knot HJ, Standen NB & Nelson MT (1998). Ryanodine receptors regulate arterial diameter and wall [Ca^{2+}] in cerebralarteries of rat via Ca^{2+}-dependent K^+ channels. *J Physiol* **508**, 211–221.

Kotlikoff MI (2003). Calcium-induced calcium release in smooth muscle: the case for loose coupling. *Prog Biophys Mol Biol* **83**, 171–191.

Kupittayanant S, Luckas MJ & Wray S (2002). Effect of inhibiting the sarcoplasmic reticulum on spontaneous and oxytocin-induced contractions of human myometrium. *Br J Obst Gynaecol* **109**, 289–296.

Laporte R, Hui A & Laher I (2004). Pharmacological modulation of sarcoplasmic reticulum function in smooth muscle. *Pharmacol Rev* **56**, 439–513.

Löhn M, Jessner W, Furstenau M, Wellner M, Sorrentino V, Haller H, Luft FC & Gollasch M (2001). Regulation of calcium sparks and spontaneous transient outward currents by RyR3 in arterial vascular smooth muscle cells. *Circ Res* **89**, 1051–1057.

Marx SO, Gaburjakova J, Gaburjakova M, Henrikson C, Ondrias K & Marks AR (2001). Coupled gating between cardiac calcium release channels (ryanodine receptors). *Circ Res* **88**, 1151–1158.

Meissner G (1994). Ryanodine receptor/Ca^{2+} release channels and their regulation by endogenous effectors. *Annu Rev Physiol* **56**, 485–508.

Meredith AL, Thorneloe KS, Werner ME, Nelson MT & Aldrich RW (2004). Overactive bladder and incontinence in the absence of the BK large conductance Ca^{2+}-activated K^+ channel. *J Biol Chem* **279**, 36746–36752.

Moriguchi S, Nishi M, Komazaki S, Sakagami H, Miyazaki T, Masumiya H, Saito SY, Watanabe M, Kondo H, Yawo H, Fukunaga K & Takeshima H (2006). Functional uncoupling between Ca^{2+} release and afterhyperpolarization in mutanthippocampal neurons lacking junctophilins. *Proc Natl Acad Sci U S A* **103**, 10811–10816.

Morimura K, Ohi Y, Yamamura H, Ohya S, Muraki K & Imaizumi Y (2006). A two step Ca^{2+} intracellular release underlies excitation-contraction coupling in mouse urinary bladder myocytes. *Am J Physiol Cell Physiol* **290**, C388–C403.

Nakai J, Imagawa T, Hakamata Y, Shigekawa M, Takeshima H & Numa S (1990). Primary structure and functional expression from cDNA of the cardiac ryanodine receptor/calcium release channel. *FEBS Lett* **271**, 169–177.

Nelson MT, Cheng H, Rubart M, Santana LF, Bonev AD, Knot HJ & Lederer WJ (1995). Relaxation of arterial smooth muscle by calcium sparks. *Science* **270**, 633–637.

Nishi M, Mizushima A, Nakagawara K & Takeshima H (2000). Characterization of human junctophilin subtype genes. *Biochem Biophys Res Commun* **273**, 920–927.

Ohi Y, Yamamura H, Nagano N, Ohya S, Muraki K, Watanabe M & Imaizumi Y (2001). Local Ca^{2+} transients and distribution of BK channels and ryanodine receptors in smooth muscle cells of guinea-pig vas deferens and urinary bladder. *J Physiol* **534**, 313–326.

Ohya S, Tanaka M, Oku T, Asai Y, Watanabe M, Giles WR & Imaizumi Y (1997). Molecular cloning and tissue distribution of an alternatively spliced variant of an A-type K^+ channel α-subunit, Kv4.3 in the rat. *FEBS Lett* **420**, 47–53.

Otsu K, Willard HF, Khanna VK, Zorzato F, Green NM & MacLennan DH (1990). Molecular cloning of cDNA encoding the Ca^{2+} release channel (ryanodine receptor) of rabbit cardiac muscle sarcoplasmic reticulum. *J Biol Chem* **265**, 13472–13483.

Park MY, Park WJ & Kim DH (1998). Expression of excitation-contraction coupling proteins during muscle differentiation. *Mol Cell* **8**, 513–517.

Pérez GJ, Bonev AD, Patlak JB & Nelson MT (1999). Functional coupling of ryanodine receptors to K_{Ca} channels in smooth muscle cells from rat cerebral arteries. *J Gen Physiol* **113**, 229–238.

Plüger S, Faulhaber J, Fürstenau M, Löhn M, Waldschütz R, Gollasch M, Haller H, Luft FC, Ehmke H & Pongs O (2000). Mice with disrupted BK channel β1 subunit gene feature abnormal Ca^{2+} spark/STOC coupling and elevated blood pressure. *Circ Res* **87**, e53–e60.

Sanders KM (2001). Mechanisms of calcium handling in smooth muscles. *J Appl Physiol* **91**, 1438–1449.

Stuyvers BD, Dun W, Matkovich S, Sorrentino V, Boyden PA & ter Keurs HE (2005). Ca^{2+} sparks and waves in canine purkinje cells: a triple layered system of Ca^{2+} activation. *Circ Res* **97**, 35–43.

Taggart MJ & Wray S (1998). Contribution of sarcoplasmic reticular calcium to smooth muscle contractile activation: gestational dependence in isolated rat uterus. *J Physiol* **511**, 133–144.

Takeshima H, Komazaki S, Hirose K, Nishi M, Noda T & Iino M (1998). Embryonic lethality and abnormal cardiac myocytes in mice lacking ryanodine receptor type 2. *EMBO J* **17**, 3309–3316.

Takeshima H, Komazaki S, Nishi M, Iino M & Kangawa K (2000). Junctophilins: a novel family of junctional membrane complex proteins. *Mol Cell* **6**, 11–22.

Takeshima H, Nishimura S, Matsumoto T, Ishida H, Kangawa K, Minamino N, Matsuo H, Ueda M, Hanaoka M, Hirose T & Numa S (1989). Primary structure and expression from complementary DNA of skeletal muscle ryanodine receptor. *Nature* **339**, 439–445.

Wang YX, Zheng YM, Mei QB, Wang QS, Collier ML, Fleischer S, Xin HB & Kotlikoff MI (2004). FKBP12.6 and cADPR regulation of Ca^{2+} release in smooth muscle cells. *Am J Physiol Cell Physiol* **286**, C538–C546.

ZhuGe R, Tuft RA, Fogarty KE, Bellve K, Fay FS & Walsh JV Jr (1999). The influence of sarcoplasmic reticulum Ca^{2+} concentration on Ca^{2+} sparks and spontaneous transient outward currents in single smooth muscle cells. *J Gen Physiol* **113**, 215–228.

Acknowledgements

This work was supported by a Grant-in-Aid for Scientific Research on Priority Areas (18059029) from The Ministry of Education, Culture, Sports, Science and Technology and by a Grant-in-Aid for Scientific Research (B) (17390045) from the Japan Society for the Promotion of Science to Y.I. This works was also supported by a Grant-in-Aid for Research on Health Sciences focusing on Drug Innovation from the Japan Health

Sciences Foundation to Y.I. We thank Dr W. R. Giles (University of Calgary, Calgary, Canada) for providing data acquisition and analysis programs and also for his critical reading of this manuscript.

Supplemental material

Online supplemental material for this paper can be accessed at:
http://jp.physoc.org/cgi/content/full/jphysiol.2007.130302/DC1
and
http://www.blackwell-synergy.com/doi/suppl/10.1113/jphysiol.2007.130302